Low cycle fatigue life prediction in shot-peened components of different geometries – Part II: Life prediction

C. You[a,*], M. Achintha[a], K.A. Soady[b], P.A.S Reed[a]

[a] Engineering Materials, Engineering and the Environment, University of Southampton, Highfield, Southampton SO17 1BJ, UK

[b] Uniper Technologies Ltd., Nottingham NG11 0EE, UK

Abstract

This study investigates the effects of shot peening on the low-cycle fatigue (LCF) performance of a low pressure steam turbine blade material. The finite element (FE) model incorporating shot peening effects, which has been introduced in Part I, has been used to predict the stabilised stress/strain state in shot-peened samples during fatigue loading. The application of this model has been extended to different notched geometries in this study. Based on the modelling results, both the Smith-Watson-Topper and Fatemi-Socie critical plane fatigue criteria have been used to predict the fatigue life of shot-peened samples (treated with two different peening intensities) with varying notched geometries. A good agreement between experiments and predictions was obtained. The application of a critical distance method considering the stress and strain hardening gradients near the shot-peened surface has been found to improve the life prediction results. The effects of surface defects on the accuracy of life predictions using the proposed method were also discussed.

Keywords: Shot peening, Fatigue life, Critical plane criteria, Finite element modelling

Nomenclature

$a_1, a_2, A_1 and\ A_2$	=	material constants
E	=	Young's modulus
k	=	material constant of the Fatemi-Socie criterion
K_t	=	stress concentration factor
L	=	depth chosen for the critical distance approach

* Corresponding author. Tel.: +44 (0) 23 8059 9450
Email address: c.you@soton.ac.uk (C. You)

N_f	=	number of cycles to failure
R	=	load ratio
R_a	=	arithmetic average roughness
FE	=	finite element
FS	=	Fatemi-Socie parameter
$\mathrm{FS_{avg}}$	=	averaged FS parameter
HCF	=	high-cycle fatigue
LCF	=	low-cycle fatigue
SWT	=	Smith-Watson-Topper parameter
$\mathrm{SWT_{avg}}$	=	averaged SWT parameter
$\Delta\gamma_{max}$	=	maximum shear strain range acting on the critical plane
$\Delta\varepsilon_n$	=	normal strain range acting on the critical plane
$\Delta\varepsilon_{xx}$	=	longitudinal strain range
$\varepsilon_\theta^{eigen}, \varepsilon_{yy}^{eigen}$ and ε_r^{eigen}	=	eigenstrain components
σ_0	=	material monotonic yield strength
$\sigma_{0.2}$	=	0.2% proof stress
σ_{m_SP}	=	mean stress level in the shot-peened condition
σ_{m_UP}	=	mean stress level in the un-peened condition
$\sigma_{n,max}$	=	maximum normal stress acting on the critical plane
σ_{xx}	=	longitudinal stress component
φ	=	angle of a plane

1. Introduction

In order to develop a comprehensive finite element (FE) modelling tool to predict the low cycle fatigue life of shot-peened metallic components, an essential first stage of the analysis is the incorporation of residual stress and strain hardening effects. An experimentally validated, eigenstrain-based FE modelling framework that can accurately incorporate the effect of residual stress and strain hardening effects has been presented in a companion paper [1]. The current paper extends the previous work [1] for predicting the LCF behaviour of a few selected shot-peened notch geometries.

There has been an increasing interest in explicitly including the effects of shot peening in life assessment methods to reduce the over-conservatism in lifing shot-peened components. In general, the conventional lifing approaches are either “total life” or “damage tolerant” approaches. Total life approaches can be used to predict the life due to microcrack nucleation and early propagation (where the crack length is typically smaller than 1 mm), which usually comprises a large part of the total fatigue life. It has been found that shot peening increases fatigue life mainly by retarding this nucleation and early propagation process in many systems [2-4]. Consequently, total life approaches are usually used as a preliminary estimation in the design process to assess the influence of shot peening on fatigue life. In contrast, damage tolerant approaches can be used to predict the remaining life of components based on the analysis of the behaviour of existing cracks. The application of damage tolerant approaches in shot-peened components has been reviewed in detail in [5]. It will not be further discussed here since the present paper focuses on total life approaches.

Among total life approaches, multiaxial fatigue criteria are thought to be most appropriate for the shot-peened state due to the multiaxial state of the residual stress pattern. One type of these approaches depends on the octahedral shear stress amplitude (or equivalently the Von Mises stress) and the hydrostatic pressure; e.g. the Sines [6] and Crossland [7] criteria. They have been found to work well in the high-cycle fatigue (HCF) regime. Another type are the critical plane criteria, such as the Dang Van [8], the Smith-Watson-Topper (SWT) [9] and the Fatemi-Socie (FS) [10] approaches. The critical plane is defined as the most severely loaded plane where cracks are expected to nucleate. Hence, critical plane criteria have been suggested to be more reliable than other criteria, since they reflect the physical nature of fatigue damage by the definition of the critical plane [11].

In terms of the range of application, the SWT and FS criteria are believed to be most robust among multiaxial fatigue criteria since they are strain-stress-based, hence can be used for both the LCF and HCF regimes. In contrast, all the other criteria (the Sines, the Crossland, and the Dang Van criteria) mentioned above are simply stress-based and are only suitable for the HCF regime where plastic deformation is small or negligible. Although in some cases the stress-based approaches can predict the LCF behaviour well [12, 13], they cannot reflect the constitutive behaviour of the material when the fatigue response changes completely from the HCF to LCF regime [11].

So far, most published studies regarding the fatigue life prediction of shot-peened components using total life approaches are confined to the HCF regime and the strain hardening effects have rarely been accounted for [12, 14, 15]. This is mainly due to the difficulties in accurately predicting the stress and strain evolutions during fatigue loading in shot-peened components when significant plastic deformation occurs in the LCF regime, especially in regions with stress concentration features. In order to achieve an accurate LCF life prediction for shot-peened components, the interaction between shot-peening-induced effects and service conditions has to be considered when applying the multiaxial fatigue criteria.

The present work aims to develop an approach which is capable of accurately predicting the LCF behaviour of shot-peened notch geometries representing the fir tree blade-disc interface of a turbine system, using both the SWT and FS critical plane criteria. As a comparison, the prediction was also carried out for un-notched samples. The novelty of this work mainly lies in the incorporation of the effects of residual stresses and strain hardening induced by shot peening on the LCF behaviour into the application of critical plane criteria. To realise this, the complex interaction between the shot peening induced effects, external loads, their corresponding stress/strain distributions and possible concomitant residual stress relaxation during service has been investigated using a FE modelling approach introduced in the companion Part I paper [1]. The application of this approach has been extended to different notched geometries in the present study. The effects of surface roughness is not considered in the current modelling work because the beneficial effects of compressive residual stresses and strain hardening usually play a dominant role when surface roughness R_a is less than 5 μm [16]. The stress/strain terms required by the critical plane criteria have been evaluated using the developed FE models, allowing for the effects of shot peening. In addition, a critical distance method has been applied to improve the accuracy of the life prediction and the effects of surface roughness were discussed. A sensitivity analysis was also carried out to investigate how the FE modelling results affected the accuracy of the life prediction.

2. Material and experimental results

2.1. Material

The microstructure and composition of the material used in the investigation, FV448 (a representative of the type of material used in low-pressure turbine blades), have been detailed in [17] and the mechanical properties have been reported in a companion paper [1].

2.2. Specimen

To simulate the effect of varying component geometries on the efficacy of shot peening, an un-notched and four different notched geometries were used. All sample notches were manufactured with a circular profile defined by diameter × depth (mm). The dimensions of the plain bend bar (PBB) specimen and the 4.5 × 1.25 notched specimen (i.e. notch diameter: 4.5 mm, notch depth: 1.25 mm) are shown in Fig. 2 (a) and (b) in Part I [1] respectively. The dimensions of the other three notched geometries used in this study were 4.5 × 3 mm, 10.5 × 1.25 mm and 10.5 × 3 mm representing different service conditions. All notched samples had the same global dimensions; 7.75 mm in width and 8.00 mm in breadth. Details of the two peening treatments (labelled as T0 and T1) used in the current study can be found in [1].

2.3. Fatigue tests

Since the maximum service temperature in LP turbines is ~ 250℃, which is outside the creep regime for this material, the service temperature was thought to have no significant effect on fatigue life. Hence, all the fatigue tests were carried out at room temperature with a sinusoidal waveform and a frequency of 20 Hz using a servo hydraulic Instron 8502. The notched and plain specimens were loaded under 3- and 4-point bend respectively with a load ratio R = 0.1. The true longitudinal strain range, $\Delta\varepsilon_{xx}$, experienced in the centre at the notch root (or in the centre of the top surface in the plain sample) was estimated using the FE model introduced in Part I [1], allowing for both effects of compressive residual stresses and strain hardening induced by shot peening.

The strain-life ($\Delta\varepsilon_{xx} - N_f$) plots for the plain sample with different surface treatments are presented in Fig. 1 (a); grinding, T0 shot peening and T0 shot peening + grinding. The grinding treatment after shot peening (T0 shot peening + grinding) was used to remove the significant lips (as shown in Fig. 2) in the edge region of the shot-peened sample which developed due to the large shear deformation occurring during the peening process. The comparison between the ground and T0 shot-peened samples indicates that shot peening is beneficial in improving fatigue life but this benefit becomes less evident with increasing $\Delta\varepsilon_{xx}$. By grinding off the edge lips generated by shot peening, the benefit of shot peening becomes even more notable, especially in the HCF regime where crack initiation dominates the total life.

Fig. 1 (a) also presents the fatigue life of the 4.5×1.25 notched sample. Three surface treatments have been considered: grinding, T1 and T0 shot peening. It can be seen that the T0 process increases the fatigue life of the 4.5×1.25 notched sample at all $\Delta\varepsilon_{xx}$ levels, including the highest range $\Delta\varepsilon_{xx} = 0.81\%$. In contrast, the T1 process gives no clear benefit in life improvement when $\Delta\varepsilon_{xx} > 0.65\%$. Fig. 1 (b) further compares the total fatigue life of the T0 shot-peened specimens with varying notch geometries (as defined in Section 2.2) in terms of $\Delta\varepsilon_{xx}$, showing that wider notches appear to have a lower fatigue life.

2.4. Crack growth characterisation

In the T0 plain sample, the edge lips were found to increase the propensity for fatigue initiation from the edges of the sample, resulting in corner crack initiation. By grinding off these edge lips, the acceleration of crack nucleation can be resisted, which explains the difference in fatigue life between the T0 and T0 shot peening + grinding conditions as shown in Fig. 1 (a). In contrast, the effect of these edge lips was much less significant in the notched sample, where centre crack initiation dominated [18]. This cracking mechanism was observed in all the notched specimens under investigation regardless of the specific notch geometry [18].

Crack growth behaviour in the 4.5×1.25 notched specimen has been investigated previously by He *et al.* [4], so relevant results are only briefly introduced here. A surface strain of $\Delta\varepsilon_{xx} = 0.69\%$ was chosen for the specimens used in this analysis. At this load level, the fatigue life of the ground sample was doubled by the T0 process while the T1 process barely gave any fatigue life benefit, as shown in

Fig. 1 (a). This situation was helpful in evaluating the interaction between the shot peening effects and external loading, this load level has therefore been examined in more detail. In both the ground and T1 shot-peened specimens, surface cracks were clearly picked up by the replica observations at ~ 50% life; from that point, these cracks developed at a constant rate until a rapid acceleration near the end of fatigue life (~ 70% - 80% life) when the main cracks coalesced. However, in the T0 condition, the cracks leading to the final fracture grew from some pre-existing microcracks introduced by shot peening. They started to grow very slowly at ~ 10% - 20% fatigue life and their growth rates did not increase dramatically until ~ 70% - 80% total life when the surface crack length was ~ 0.5 - 1.0 mm. This retardation of the short crack growth process was thought to be the main contribution to the improvement of fatigue life in this specific system.

4. Life prediction approaches

According to Fig. 1, the actual local strain range ($\Delta\varepsilon_{xx}$) cannot uniquely characterise the fatigue life data for conditions with different surface treatments and geometries, even when the effects of compressive residual stresses and strain hardening are taken into account. This is thought to be a result of the mean stress level or the stress/strain ratios within the surface layer during fatigue loading being changed by shot peening, compared with the un-peened condition [19, 20]. Consequently, in order to predict the fatigue life of shot-peened components using total life approaches, a damage parameter applying to situations with varying loading amplitudes and mean stress levels should be selected instead of the local strain range. According to the review discussed in Section 1, both the Smith-Watson-Topper (SWT) and the Fatemi-Socie (FS) damage parameters were selected in the present study to account for shot peening effects.

4.1. Critical plane criteria

4.1.1. The Smith-Watson-Topper (SWT) criterion

Smith *et al.* [9] proposed a damage parameter governing the uniaxial fatigue of metals. It was then extended by Socie [21] to a critical plane multiaxial fatigue criterion, as defined by Equation 1, where

$\sigma_{n,max}$ and $\Delta\varepsilon_n$ are the maximum stress and the strain range perpendicular to the critical plane during one cycle; the critical plane is defined as the one with the maximum damage accumulation. The SWT parameter can be related to fatigue life using a general format described by Equation 2, where A_1, A_2, a_1 and a_2 are material constants and can be determined by calibration tests. This criterion is most suitable for Mode I cracks which are developed by high tensile stresses.

$$\mathrm{SWT} = \frac{1}{2}\sigma_{n,max}\Delta\varepsilon_n \qquad (1)$$

$$\frac{1}{2}\sigma_{n,max}\Delta\varepsilon_n = A_1 {N_f}^{a_1} + A_2 {N_f}^{a_2} \qquad (2)$$

4.1.2. The Fatemi-Socie (FS) criterion

For Mode II cracks growing on planes with high shear stresses, Fatemi and Socie [10] suggested a damage parameter which was expressed as a function of the maximum shear strain range, $\Delta\gamma_{max}$, and the maximum normal stress acting on the maximum shear strain plane over one cycle, $\sigma_{n,max}$, as described by Equation 3, where σ_0 is the material monotonic yield strength and k is a material constant. The value of k can be determined by fitting uniaxial fatigue data to torsion fatigue data. In the present study, $k = 1$ has been used as an initial estimate due to the lack of relevant experimental data, as suggested in [11]. The FS parameter can be related to fatigue life using the general format described by Equation 4.

$$FS = \frac{\Delta\gamma_{max}}{2}\left(1 + k\frac{\sigma_{n,max}}{\sigma_0}\right) \qquad (3)$$

$$\frac{\Delta\gamma_{max}}{2}\left(1 + k\frac{\sigma_{n,max}}{\sigma_y}\right) = A_1 {N_f}^{a_1} + A_2 {N_f}^{a_2} \qquad (4)$$

4.2. Finite element modelling

Using the eigenstrains-based modelling approach [1] that has been developed by the authors to incorporate the compressive residual stress and strain hardening effects caused by shot peening. The residual stress distributions in the shot-peened plain and notched (4.5 × 1.25) samples were first reconstructed and relevant modelling results are shown in Fig. 3 (a). All the presented residual stress profiles (except the T1 notched case) have been validated with experimental data (see Fig. 8 and 9 in Part I [1]).

Then, the validated modelling approach was extended to different notched geometries (as presented in Section 2.2) treated with the T0 shot peening process: The modelled residual stress distributions are shown in Fig. 3 (b). In the modelling work, the eigenstrain component tangential to the notch curvature, $\varepsilon_{\theta}^{eigen}$, was evaluated using an assumption described by Equation 5, where ε_{yy}^{eigen} is the eigenstrain component in the transverse direction and c is the ratio between the eigenstrains in the longitudinal direction and the transverse direction; details of this analysis is presented in a companion paper [1]. The value of c was numerically determined to be 1.58 for the 4.5 × 1.25 notched geometry and the corresponding value of other notched geometries, 4.5 × 3, 10.5 × 1.25 and 10.5 × 3, were numerically determined to be 1.48, 1.27 and 1.21 respectively. Although this empirical method may need further validation, as it can be seen from the results presented in this paper, the model predictions at least consistent with the experimental results of the test specimens analysed in the current study. The third eigenstrain component, ε_{r}^{eigen}, which is perpendicular to the notch curvature, was calculated using Equation 6, considering volume conservation in plastic deformation.

$$\varepsilon_{\theta}^{eigen} = c\ \varepsilon_{yy}^{eigen} \qquad (5)$$

$$\varepsilon_{r}^{eigen} = -(\varepsilon_{\theta}^{eigen} + \varepsilon_{yy}^{eigen}) \qquad (6)$$

In addition to the residual stress effects, the strain hardening effects were also accounted for in the developed model by increasing the local material yield strength based on EBSD measurements, as introduced in Part I [1].

This modelling approach was validated by showing it could satisfactorily predict the stress/strain evolution during fatigue loading [1]. This is helpful to the application of fatigue criteria in assessing fatigue life by determining the required stress/strain terms allowing for shot peening effects.

4.3. Life prediction procedure

Since all the cracks were observed to initiate from the surface [22], the surface stress and strain data during the first cycle were extracted from the modelling results based on corresponding geometric features and shot peening effects. A plane was defined in terms of φ, the angle measured counter-clockwise from the x axis of the specimen (i.e. the longitudinal direction) to the normal vector on an inclined plane. The normal stress, normal strain and shear strain on the plane were calculated using the extracted modelling results, according to Equations 7 - 9 respectively. To determine the critical plane, planes were checked at all angles between $-90^{\circ} < \varphi < 90^{\circ}$ with an interval of 1°. The predicted critical planes using the SWT and FS criteria for the T0 shot-peened 4.5×1.25 notched specimen when $\Delta\varepsilon_{xx} = 0.69\%$ are $\varphi = 0^{\circ}$ and $\pm 45^{\circ}$ respectively. Similar results were obtained for other conditions with different geometries, peening intensities or load levels, so they are not presented here for brevity.

$$\sigma_n = \frac{\sigma_{xx}+\sigma_{yy}}{2} + \frac{\sigma_{xx}-\sigma_{yy}}{2}\cos 2\varphi + \tau_{xy}\sin 2\varphi \qquad (7)$$

$$\varepsilon_n = \frac{\varepsilon_{xx}+\varepsilon_{yy}}{2} + \frac{\varepsilon_{xx}-\varepsilon_{yy}}{2}\cos 2\varphi + \frac{\gamma_{xy}}{2}\sin 2\varphi \qquad (8)$$

$$\gamma = -\sin 2\varphi \left(\varepsilon_{xx} - \varepsilon_{yy}\right) + \gamma_{xy}\cos 2\varphi \qquad (9)$$

The calibration curves were determined based on Equations 2 and 4, which are generally suggested to be fitted to the fatigue life data of simple smooth specimens under uniaxial loading (i.e. the calibration data) [9, 10]. But due to the lack of relevant data in the present study, the bending fatigue life of ground samples were regarded as the calibration data instead. The SWT and FS parameters for the ground sample at different load levels were evaluated at the sample surface using the FE model without shot peening effects. Surface modifications (i.e. roughness, residual stresses and strain hardening) introduced by grinding were neglected in the modelling work since it was found that their effects were limited in the LCF regime in the present system [4, 23].

The obtained calibration curves for the SWT and the FS criteria are shown in Fig. 4 (a) and (b) respectively. It is noted that this fitting work was carried out for the plain and notched samples separately due to their different crack nucleation and growth mechanisms as explained in Section 2.4. Although the critical plane criteria are typically used to predict the crack initiation and early propagation life, the total fatigue life data were directly used to simplify the life prediction process. This simplification was thought to have little influence on the accuracy of the predicted results, because the crack initiation and early propagation process took at least ~ 70% - 80% of the total life as discussed in Section 2.4.

In the final step, the calibration curves shown in Fig. 4 were used to predict the fatigue life of shot-peened samples at given load levels in terms of the corresponding damage parameter, which was determined using the developed FE model incorporating shot peening effects.

It has been suggested by some references [24] that using the stabilised stress/strain state can lead to a more accurate life prediction. However, the FE approach applied in the present study is only capable of predicting the stress/strain evolution during the quasi-static loading stage (the first cycle) without considering the cyclic behaviour [1]. This simplification was assumed to have negligible influence on the accuracy of life prediction for the notched sample, because the experimental observation suggested residual stress relaxation at the notch root only occurred during the first cycle owing to the high constraints exerted by the notch geometry with no further logarithmic relaxation though life [23]. As for the plain sample, although there was no direct experimental validation on how the residual stress relaxed beyond the first cycle, based on the notched results in the light of the material cyclic behaviour, it is reasonable to assume that the relaxation is most significant during the quasi-static loading stage [25, 26] such that the applied simplification was used as an appropriate approximation.

4.4. Life prediction results

The predicted fatigue life using the SWT and FS criteria are shown in Fig. 5 and Fig. 6 respectively, and compared with corresponding experimental results. Despite the evident difference between the predicted critical planes (Section 4.3), the predicted fatigue life using the two criteria are similar. Regarding the plain sample, the predicted results are more consistent with the condition without edge lips (T0 shot peening + grinding); most predicted data fall within the factor of two error band. In contrast, in the condition with retained edge lips (T0), although the fatigue life data for less than 10^5 cycles were still accurately predicted, the life data between 10^5 and 10^6 cycles were significantly overestimated. As for the notched sample, both criteria have resulted in an acceptable prediction for specimens with different conditions (different peening intensities and notch geometries) where most predicted data points are located within the factor of three error band.

5. Discussion

The stress and strain states at safety critical regions during fatigue loading were directly predicted using the FE model. This approach is believed to be more accurate than the simple stress superposition method applied by many researchers [13, 14, 27, 28] because it ensures global stress equilibrium, strain compatibility and also matches the boundary conditions.

5.1. Improvement of the life prediction using a critical distance approach

The results shown in Fig. 5 and Fig. 6 were obtained simply using the surface stress/strain data. Nevertheless, for shot-peened samples, the compressive residual stress profile with a typical “hook” shape may result in a high gradient of the stress distribution beneath the surface when external loads are applied. Furthermore, strain hardening may also influence the subsurface stress/strain distribution during fatigue loading due to the changed local yield stress. These effects may significantly affect the total fatigue life by influencing the crack growth behaviour [4]. Hence, the life prediction results might be improved if the stress/strain state within a layer near the surface was taken into account, rather than simply using the surface stress/strain data.

To investigate the effects of shot peening on the stress state near the sample surface during fatigue loading, the reduction in mean stress caused by the T0 shot peening in the 4.5 × 1.25 notched sample at varying $\Delta\varepsilon_{xx}$ levels was calculated. $\Delta\varepsilon_{xx}$ was determined using the FE model with and without shot peening effects for the peened and un-peened samples respectively. The mean stress profile was calculated by averaging the maximum and minimum stress profiles within one cycle, which was obtained from the modelling results. To better quantify the reduced mean stress, the degree of the mean stress reduction is defined using Equation 10, where σ_{m_SP} and σ_{m_UP} are the mean stress levels in the peened and un-peened conditions respectively.

$$\text{Reduced mean stress (\%)} = \frac{\sigma_{m\_SP} - \sigma_{m\_UP}}{\sigma_{m\_UP}} \times 100\% \qquad (10)$$

Relevant results are shown in Fig. 7. It can be seen that the reduction of mean stress is confined to within a depth of ~ 0.35 mm (similar to the depth of the compressive residual stress profile shown in Fig. 3) regardless of the $\Delta\varepsilon_{xx}$ level. But the degree of the mean stress reduction becomes less evident with increasing $\Delta\varepsilon_{xx}$ levels. Similar trends have also been obtained for the T0 plain and T1 notched samples which are not presented here for brevity. This trend is consistent with that shown in Fig. 1; the benefit of shot peening in improving fatigue life is less significant at higher load levels with higher $\Delta\varepsilon_{xx}$. Hence, it seems that the benefits of shot peening in improving fatigue life can be potentially attributed to mean stress reductions.

To account for the mean stress effects, a critical distance approach [29] has been applied in the present study to calculate an engineering quantity representative of the real damage accumulated in the fatigue process zone. Referring to the definition of critical distances, the SWT and FS parameters were averaged over a depth of L = 0.35 mm and 0.20 mm for the T0 and T1 conditions respectively, as described by Equation 11. This depth, indicating the range of shot peening effects, was determined according to the mean stress profiles shown in Fig. 7.

$$\mathrm{SWT_{avg}} = \frac{\int_0^L SWT(z)\,dz}{L}, \ \ \mathrm{FS_{avg}} = \frac{\int_0^L FS(z)\,dz}{L} \qquad (11)$$

Fig. 8 and Fig. 9 show the life prediction results using the averaged damage parameters $\mathrm{SWT_{avg}}$ and $\mathrm{FS_{avg}}$ instead of the surface parameters SWT and FS. Compared with the results shown in Fig. 5 and Fig. 6, the application of the defined critical distance has effectively improved the accuracy of the life prediction, especially for the notched samples; most results are now located within the factor of two error band. On the other hand, the data points between 10^5 and 10^6 cycles for the plain sample with edge lips are still overestimated.

5.2. The effects of initial defects

In shot-peened plain samples, crack initiation was always observed at the corner where edge lips existed [22]. These edge lips acted as stress concentration raisers which significantly accelerated the crack initiation life. This effect tended to be more significant for longer fatigue lives under low load levels, where crack initiation was more dominant determining in total life. However, the detrimental effect of edge lips was not considered in the life prediction process applied in the present study. Hence, the fatigue life data of the shot-peened plain sample have been significantly overestimated when N_f is between 10^5 and 10^6 cycles, as shown in Fig. 5 (a), Fig. 6 (a), Fig. 8 (a) and Fig. 9 (a). By removing these edge lips by further grinding (i.e. the data points labelled as "Plain_T0 + ground"), this detrimental effect was significantly reduced, which made the experimental and predicted life data more consistent.

In contrast, centre crack initiation dominated in shot-peened notched samples. The edge lips were therefore found to have much less effect on the fatigue life of notched samples. The difference in crack initiation sites between the shot-peened plain and notched samples can be explained by consideration of the FE-predicted tensile stress distribution across the sample from the centre (y = 0 mm) to the edge (y = 4 mm) when they are loaded beyond the elastic limit, as shown in Fig. 10. The σ_{xx} in the plain sample is more evenly distributed than in the notched sample, which means that defects at the edges of the plain sample are more likely to promote crack initiation compared with the notched sample. Hence, in any practical application, consideration must be given to removing any shear lips resulting from the peening process when there is no other geometric stress concentration in the treated area.

In addition to the edge lips, shot peening may increase surface roughness or introduce some surface microcracks due to a high peening intensity. These detrimental effects were not considered in the life prediction process in the present study. This was because the benefits of shot peening resulting from compressive residual stresses and strain hardening dominated in most cases [2, 4, 22, 30]. However, in conditions where an excessive peening intensity is applied or compressive residual stresses relax rapidly (i.e. where high stresses are applied to a region of low constraint), a more advanced life assessment approach considering the detrimental effects of the imperfect surface should be applied instead, otherwise the fatigue life would be overestimated.

5.3. Comparison between the SWT and FS critical plane criteria

For the shot-peened notched samples, both the SWT and FS criteria have generated satisfactory life prediction results. However, the predicted crack orientations are quite different between the two criteria; $\varphi = 0^{\circ}$ and $\pm 45^{\circ}$ using the SWT and FS criteria respectively. This discrepancy is not unexpected and often exists in the application of critical plane models [31, 32], mainly due to the different mechanisms assumed between different critical plane criteria. In order to ensure a good accuracy of the life prediction, it has been suggested that the applied critical plane criterion should be chosen according to the specific cracking mode. However, this can be difficult due to the complexity of the cracking mechanism. The cracking mode usually depends on the internal defects [4, 15], the material type and external loads [13, 36] and tends to become more complex in shot-peened components. Consequently, simply using a single fatigue criterion apparently cannot describe all the possible situations, which may result in an unsatisfactory prediction of the crack orientation.

Despite many difficulties in accurately predicting the cracking mode in different systems, the critical plane criteria have been demonstrated to be relatively robust in predicting the fatigue life. This is supported by others' work [31, 32] and the results obtained in the present study. In the present case, the relation between $\mathrm{SWT_{avg}}$ and $\mathrm{FS_{avg}}$ is shown in Fig. 11, which demonstrates an approximately proportional relation between the two damage parameters obtained for all the investigated notched samples. This indicates that the predicted damage accumulation trends during fatigue loading using the SWT and FS criteria are similar despite their different definitions of the damage parameter, which is consistent with the conclusion made by Jiang *et al*. [32]. Therefore, in conditions where microstructural defects do not significantly accelerate crack initiation and early propagation, acceptable life prediction results can be expected using either criteria as long as the macroscopic stress/strain evolutions at critical regions during fatigue loading are accurately predicted to make sure that the overall damage accumulation in the specimen is reasonably determined.

5.4. Sensitivity analysis

Although the SWT and FS critical plane criteria seem work well in the current system, a sensitivity analysis is necessary to assess the influence of the FE modelling results on the accuracy of life predictions. This analysis is an extension of a previous sensitivity analysis presented in Part I [1], which investigated how the accuracy of the input data of the FE model (i.e. the initial residual stress and strain hardening profiles) affected the prediction of residual stress relaxation. In the present study, the parametric analysis matrix was same with the one used in Part I (see Table 3 in Part I [1]), which was composed of varying eigenstrain and initial true plastic strain profiles labelled as *a*, *b* and *c* (see Table 2 in Part I [1]); the profiles with label *b* were the baseline profiles and the ones labelled as *a* and *c* reflected the experimental error range reported in [17].

The FE models with varying eigenstrain and initial true plastic strain profiles were used to predict the fatigue life of the T0 shot-peened 4.5 × 1.25 notched specimen at two differing load levels ($\Delta\varepsilon_{xx}$ = 0.69% and 0.81%), following the life prediction procedure outlined in Section 4.3. The results for the SWT criterion are shown in Fig. 12; the results for the FS criteria are omitted since very similar results with the SWT criterion were obtained. From Fig. 12 (a), it can be seen that there is no clear effect of the variation in the initial strain hardening profiles, which is consistent with the sensitivity analysis of residual stress relaxation as detailed in [1]. In Fig. 12 (b), although varying initial residual stress profiles result in some variation in the predicted fatigue life, all the predicted life points are still within the factor of two error band. Hence, an overall conclusion can be made that the accuracy of the developed life prediction approach is more sensitive to the initial residual stresses than to the initial plastic strain. However this analysis also shows that a typical experimental error range is unlikely to result in an unacceptable difference in the final life prediction results via this methodology.

6. Conclusions

- By allowing for the effects of shot peening on local stress-strain evolution in terms of compressive residual stresses and strain hardening, the SWT and FS criteria have been demonstrated to accurately predict the LCF life of shot-peened specimens (especially those with stress concentration features). The stress/strain status during fatigue loading in shot-peened specimens can be effectively evaluated using an FE modelling approach.

- Shot peening effectively reduces the mean stress level within a surface layer during fatigue loading. The degree of this reduction becomes less significant at high load levels, giving reduced benefit from shot peening in terms of improving fatigue life. In this case, the principal benefit of shot peening can be linked to effective reductions in mean stress level. Application of the critical distance method to account for the stress/strain gradients near the surface can further improve the life prediction results using the SWT and FS criteria.

- Surface defects introduced by shot peening may significantly reduce the crack initiation time. In such situations, their detrimental effects need to be accounted for in the lifing procedure. Otherwise the fatigue life may be inappropriately overestimated.

- The crack orientation is more difficult to accurately predict than overall fatigue life. This is mainly ascribed to the inconsistency between the theoretical assumption of the critical plane and the complexity in the real cracking mechanism. Nevertheless, the predicted crack orientation seems not to play a decisive role in the accuracy of life prediction in this case.

- The predicted fatigue life using the developed FE-based approach is more sensitive to the initial residual stress profile than to the initial strain hardening profile. But as long as the initial input data are within a reasonable experimental error range, the accuracy of the predicted fatigue life would not be unacceptably affected.

Acknowledgements

Financial support from China Scholarship Council, the Engineering and Physical Sciences Research Council (EP/K503150/1), and Uniper Technologies Ltd. is gratefully acknowledged. The authors also acknowledge the support of the University of Southampton for access to its IRIDIS4 High Performance Computing Facility.

All data supporting this study are openly available from the University of Southampton repository at http://eprints.soton.ac.uk/391080/ (http://dx.doi.org/10.5258/SOTON/391080 will be used instead when this DOI is registered after the acceptance of this paper).

Reference

1. You C, Achintha M, Soady KA, Smyth N, Fitzpatrick ME, Reed PAS (Submitted) Low cycle fatigue life prediction in shot-peened components of different geometries – Part I: Residual stress relaxation. *Fatigue & Fracture of Engineering Materials & Structures*.
2. Rios ERdl, Walley A, Milan MT, Hammersley G (1995) Fatigue crack initiation and propagation on shot-peened surfaces in A316 stainless steel. *International Journal of Fatigue*. **17**: 493-499.
3. Guagliano M, Vergani L (2004) An approach for prediction of fatigue strength of shot peened components. *Engineering Fracture Mechanics*. **71**: 501-512.
4. He BY, Soady KA, Mellor BG, Harrison G, Reed PAS (2016) Fatigue crack growth behaviour in the LCF regime in a shot peened steam turbine blade material. *International Journal of Fatigue*. **82**: 280-291.
5. Soady KA, Mellor BG, Reed PAS (2013) Life assessment methodologies incoroporating shot peening process effects: mechanistic consideration of residual stresses and strain hardening Part 2 - approaches to fatigue lifing after shot peening. *Materials Science and Technology*. **29**: 652-664.
6. Sines G, Waisman JL, Dolan TJ (1959) *Metal fatigue*. McGraw-Hill.
7. Crossland B (1956) Effect of large hydrostatic pressures on the torsional fatigue strength of an alloy steel. *Proc Int Conf on Fatigue of Metals*. Institution of Mechanical Engineers London.
8. Van KD (1971) Sur la résistance à la fatigue des métaux.
9. Smith KN, Topper TH, Watson P (1970) A stress-strain function for the fatigue of metals. *Journal of Materials*. **5**: 767-778.
10. Fatemi A, Socie DF (1988) A critical plane approach to multiaxial fatigue damage including out-of-phase loading. *Fatigue & Fracture of Engineering Materials & Structures*. **11**: 149-165.
11. Fatemi A, Shamsaei N (2011) Multiaxial fatigue: An overview and some approximation models for life estimation. *International Journal of Fatigue*. **33**: 948-958.
12. Liu J, Pang M (2012) Fatigue life prediction of shot-peened steel. *International Journal of Fatigue*. **43**: 134-141.

13. Benedetti M, Fontanari V, Bandini M (2011) A simplified and fast method to predict plain and notch fatigue of shot peened high-strength aluminium alloys under reverse bending. *Surface and Coatings Technology*.
14. Cuellar SD, Hill MR, DeWald AT, Rankin JE (2012) Residual stress and fatigue life in laser shock peened open hole samples. *International Journal of Fatigue*. **44**: 8-13.
15. Prasannavenkatesan R, Zhang J, McDowell DL, Olson GB, Jou H-J (2009) 3D modeling of subsurface fatigue crack nucleation potency of primary inclusions in heat treated and shot peened martensitic gear steels. *International Journal of Fatigue*. **31**: 1176-1189.
16. Soady KA (2013) Life assessment methodologies incoroporating shot peening process effects: mechanistic consideration of residual stresses and strain hardening Part 1 - effect of shot peening on fatigue resistance. *Materials Science and Technology*. **29**: 637-651.
17. Soady KA, Mellor BG, West GD, Harrison G, Morris A, Reed PAS (2013) Evaluating surface deformation and near surface strain hardening resulting from shot peening a tempered martensitic steel and application to low cycle fatigue. *International Journal of Fatigue*. **54**: 106-117.
18. Soady KA (2013) Reducing conservatism in life assessment approaches: Industrial steam turbine blade to disc interfaces and the shot peening process. *University of Southampton*.
19. Cláudio RA, Silva JM, Branco CM, Byrne J (2008) Fatigue life prediction of shot peened components. *Ciência & Tecnologia dos Materiais*. **20**: 99-105.
20. Xiang Y, liu Y (2010) Mechanism modelling of shot peening effect on fatigue life prediction. *Fatigue & Fracture of Engineering Materials & Structures*. **33**: 116-125.
21. Socie DF (1987) Multiaxial Fatigue Damage Models. *Journal of Engineering Materials and Technology*. **109**: 293-298.
22. He BY, Soady KA, Mellor BG, Morris A, Reed PAS (2013) Effects of shot peening on short crack growth rate and resulting low cycle fatigue behaviour in low pressure turbine blade material. *Materials Science and Technology*. **29**: 788-796.
23. Soady KA, Mellor BG, Shackleton J, Morris A, Reed PAS (2011) The effect of shot peening on notched low cycle fatigue. *Materials Science and Engineering: A*. **528**: 8579-8588.
24. Benedetti M, Fontanari V, Bandini M, Taylor D (2014) Multiaxial fatigue resistance of shot peened high-strength aluminum alloys. *International Journal of Fatigue*. **61**: 271-282.
25. Dalaei K, Karlsson B, Svensson LE (2011) Stability of shot peening induced residual stresses and their influence on fatigue lifetime. *Materials Science and Engineering: A*. **528**: 1008-1015.
26. Song X, Liu WC, Belnoue JP, et al. (2012) An eigenstrain-based finite element model and the evolution of shot peening residual stresses during fatigue of GW103 magnesium alloy. *International Journal of Fatigue*. **42**: 284-295.
27. Terres MA, Laalai N, Sidhom H (2012) Effect of nitriding and shot-peening on the fatigue behavior of 42CrMo4 steel: Experimental analysis and predictive approach. *Materials & Design*. **35**: 741-748.
28. Palin-Luc T, Coupard D, Dumas C, Bristiel P (2011) Simulation of multiaxial fatigue strength of steel component treated by surface induction hardening and comparison with experimental results. *International Journal of Fatigue*. **33**: 1040-1047.
29. Taylor D (2008) The theory of critical distances. *Engineering Fracture Mechanics*. **75**: 1696-1705.
30. Wagner L (1999) Mechanical surface treatments on titanium, aluminum and magnesium alloys. *Materials Science and Engineering: A*. **263**: 210-216.
31. Araujo JA, Nowell D (2002) The effect of rapidly varying contact stress fields on fretting fatigue. *International Journal of Fatigue*. **24**: 763-775.
32. Jiang Y, Hertel O, Vormwald M (2007) An experimental evaluation of three critical plane multiaxial fatigue criteria. *International Journal of Fatigue*. **29**: 1490-1502.

33. He BY, Katsamenis OL, Mellor BG, Reed PAS (2015) 3-D analysis of fatigue crack behaviour in a shot peened steam turbine blade material. *Materials Science and Engineering: A*. **642**: 91-103.

Figures

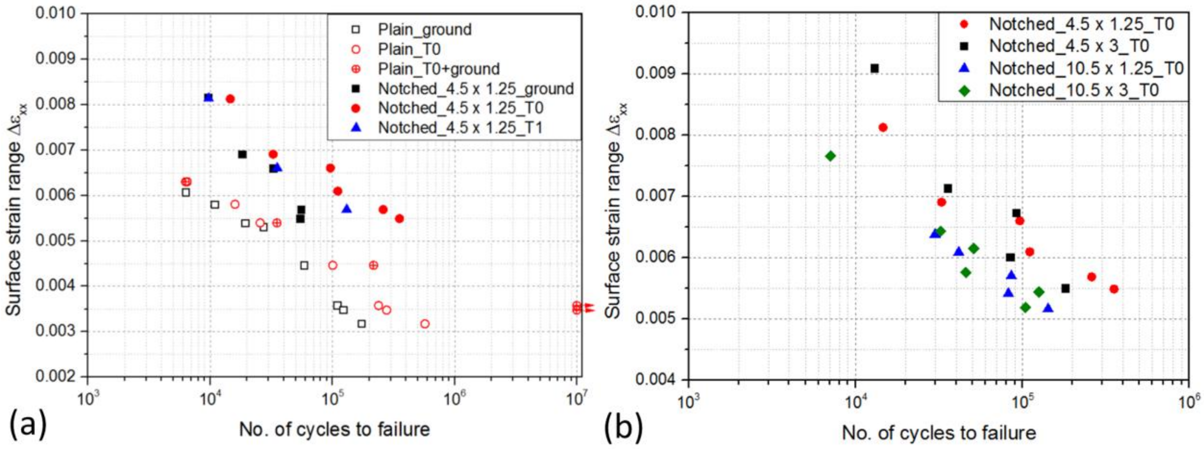

Fig. 1: Strain-life comparison (a) between the plain and notched (4.5 × 1.25) samples with different surface conditions, and (b) between T0 shot-peened notched samples with different notch geometries (fatigue life data reported in [22, 23] were re-plotted using the FE model incorporating shot peening effects).

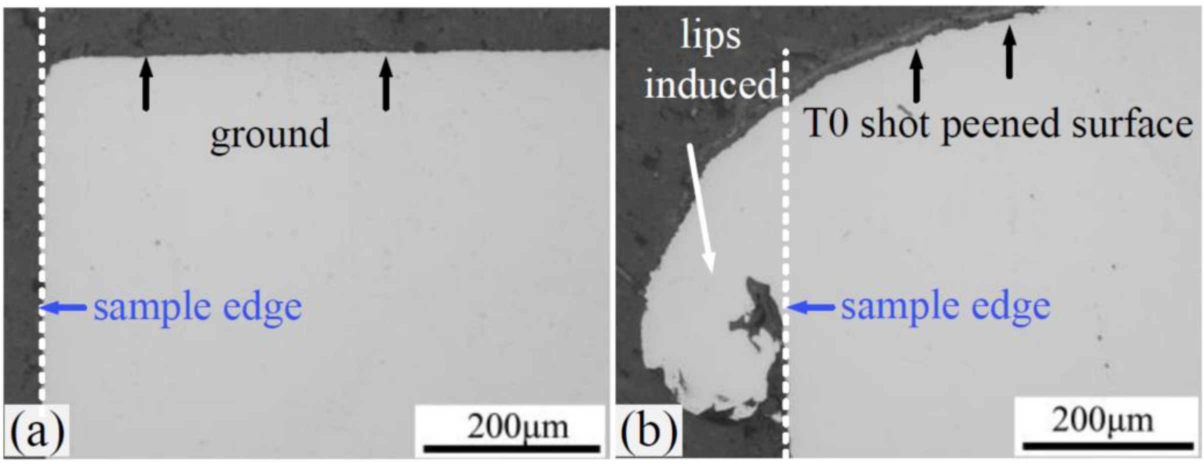

Fig. 2: Shot peening lips illustration shear deformation in the edge region in the (a) ground and (b) T0 shot-peened condition. After He *et al.* [33].

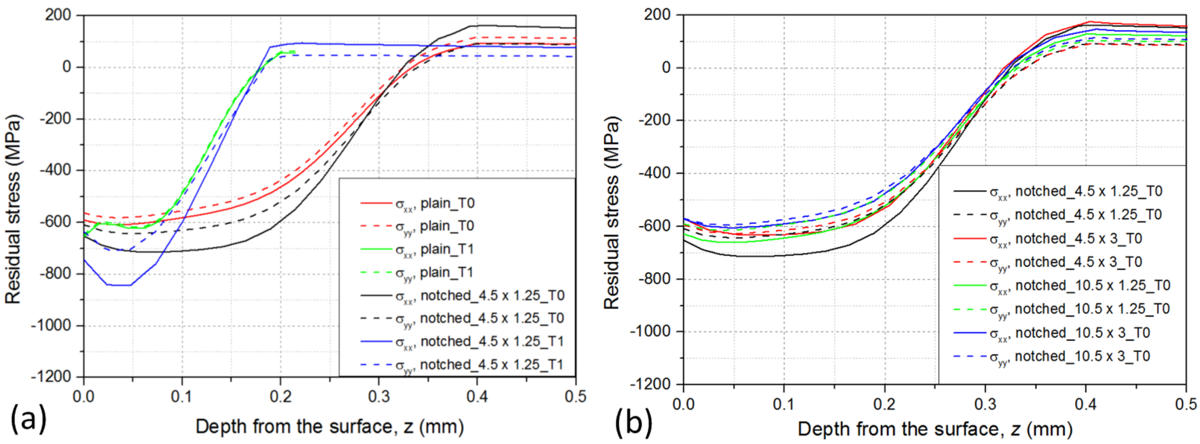

Fig. 3: Modelled residual stress distributions (a) in the T0 & T1 shot-peened plain and notched (4.5 × 1.25) samples and (b) in the T0 shot-peened notched samples with different notch geometries.

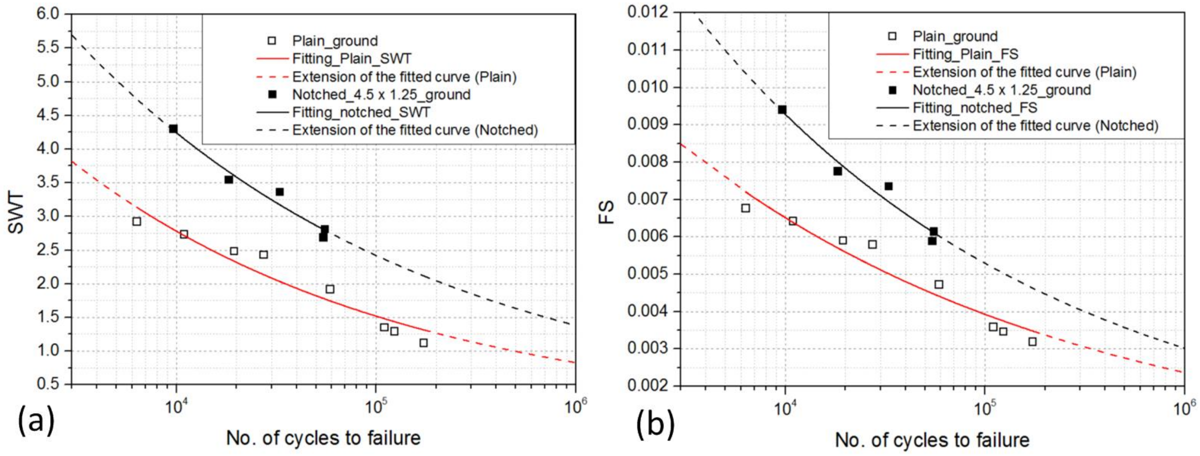

Fig. 4: Fitted calibration curves based on the fatigue life of ground samples for the (a) SWT and (b) FS criteria using the surface stress/strain data.

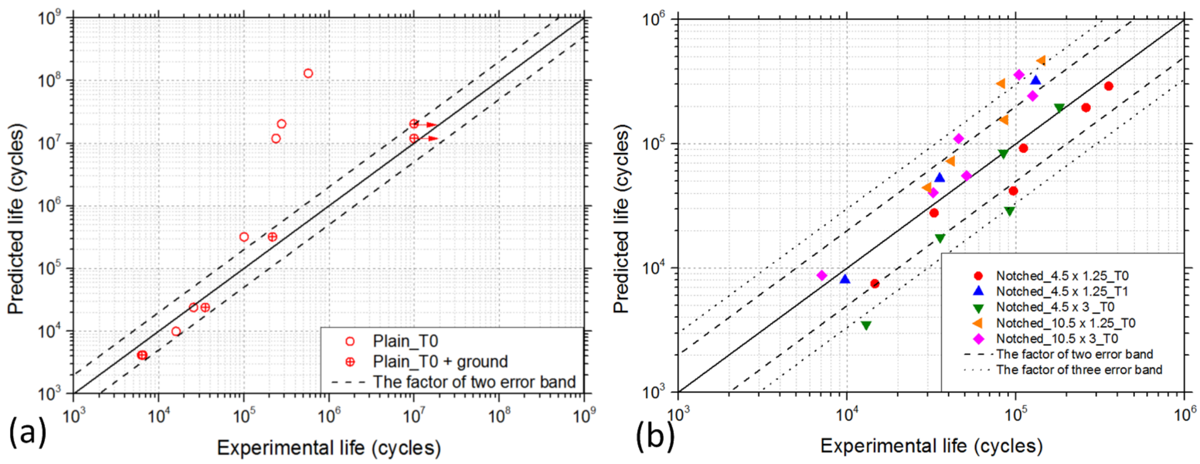

Fig. 5: Life prediction using the surface SWT parameter for the (a) plain and (b) notched samples.

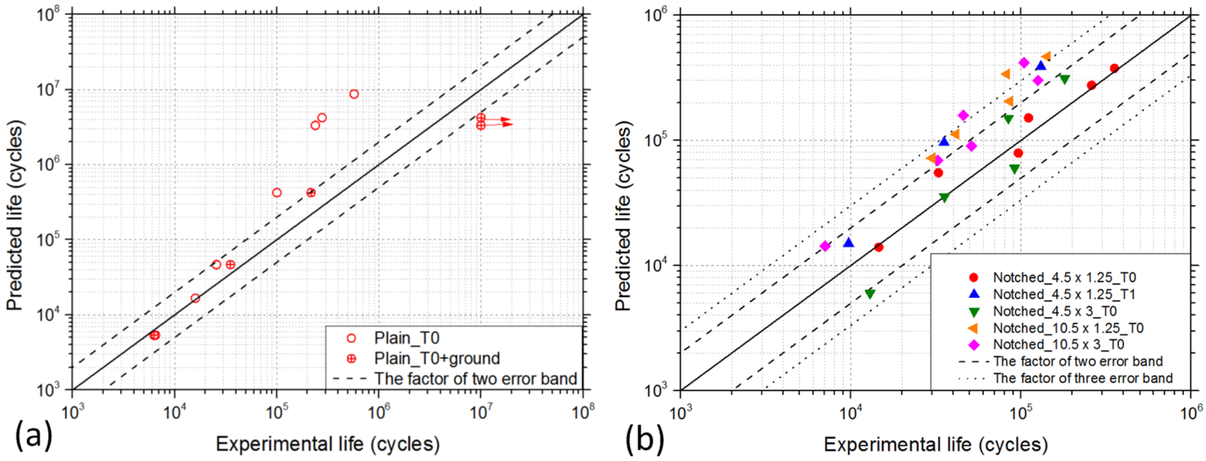

Fig. 6: Life prediction using the surface FS parameter for the (a) plain and (b) notched samples.

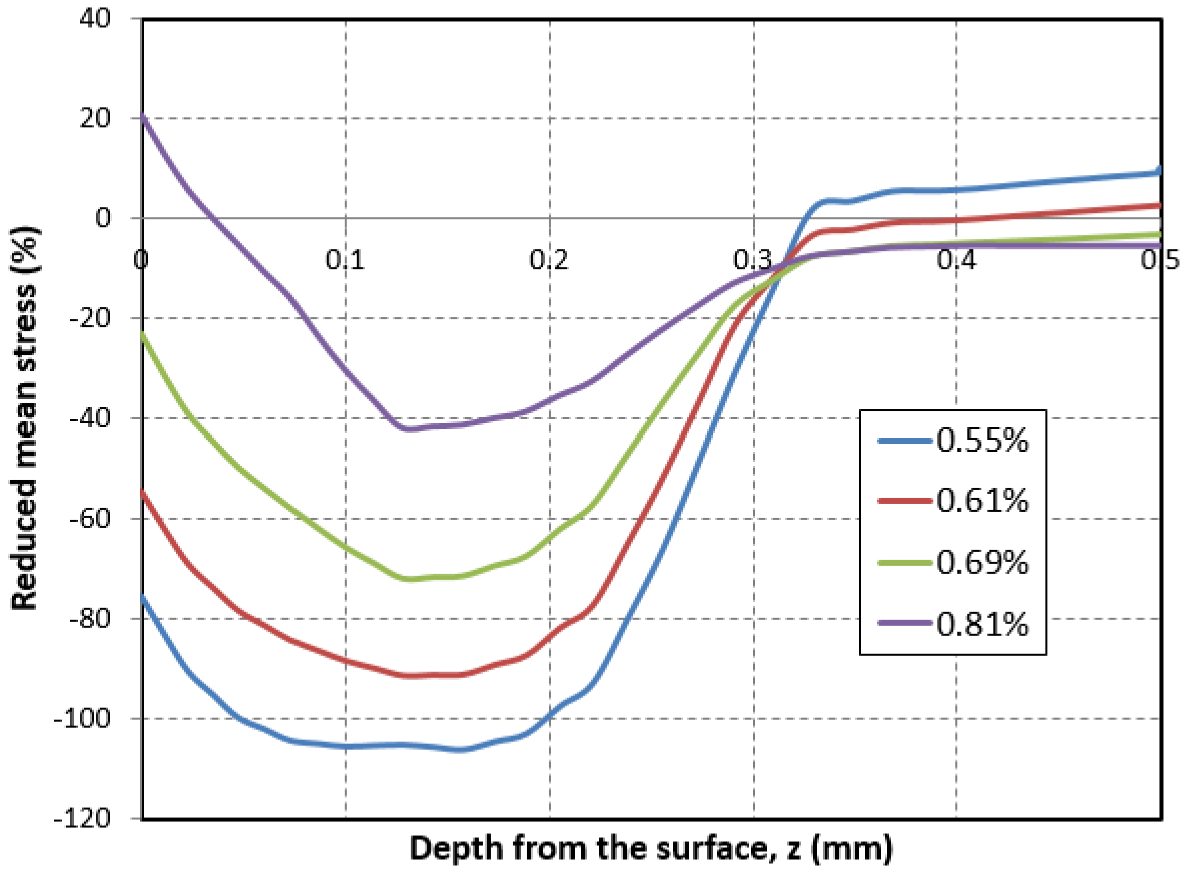

Fig. 7: The degree of the reduction in mean stress levels by the T0 shot peening in notched samples (4.5 × 1.25) at different $\Delta\varepsilon_{xx}$ levels.

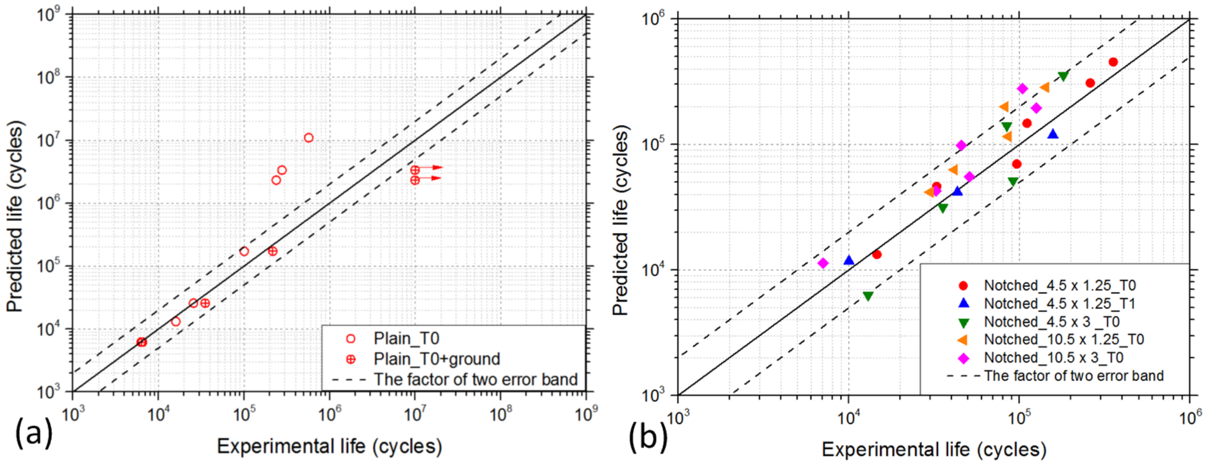

Fig. 8: Life prediction using the averaged SWT parameter for the (a) plain and (b) notched samples.

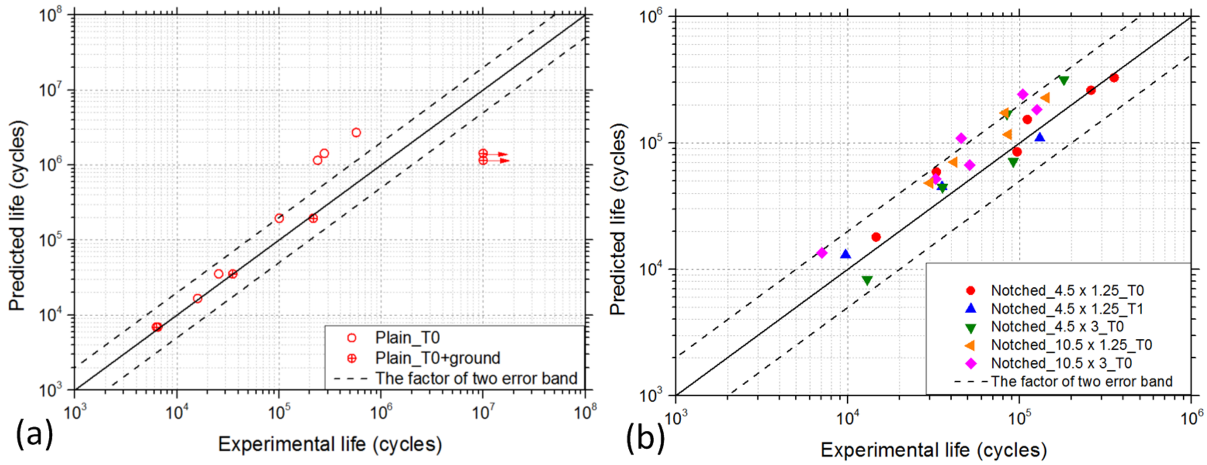

Fig. 9: Life prediction using the averaged FS parameter for the (a) plain and (b) notched samples.

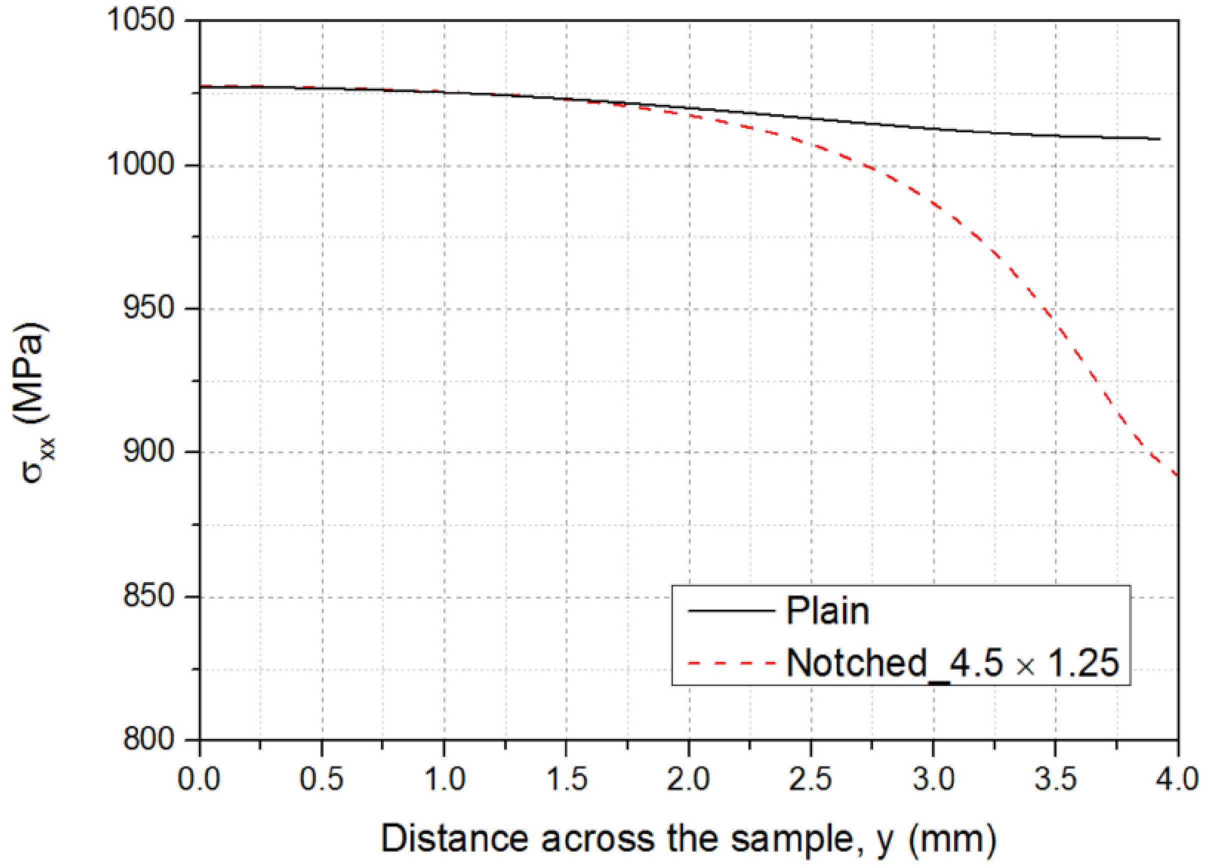

Fig. 10: Comparison of tensile stress ($\boldsymbol{\sigma_{xx}}$) distribution under maximum load in the 4.5 × 1.25 notched sample tested at $\boldsymbol{\sigma_{nom}}$ = 1034 MPa with that in the plain sample tested at the same maximum $\boldsymbol{\sigma_{xx}}$.

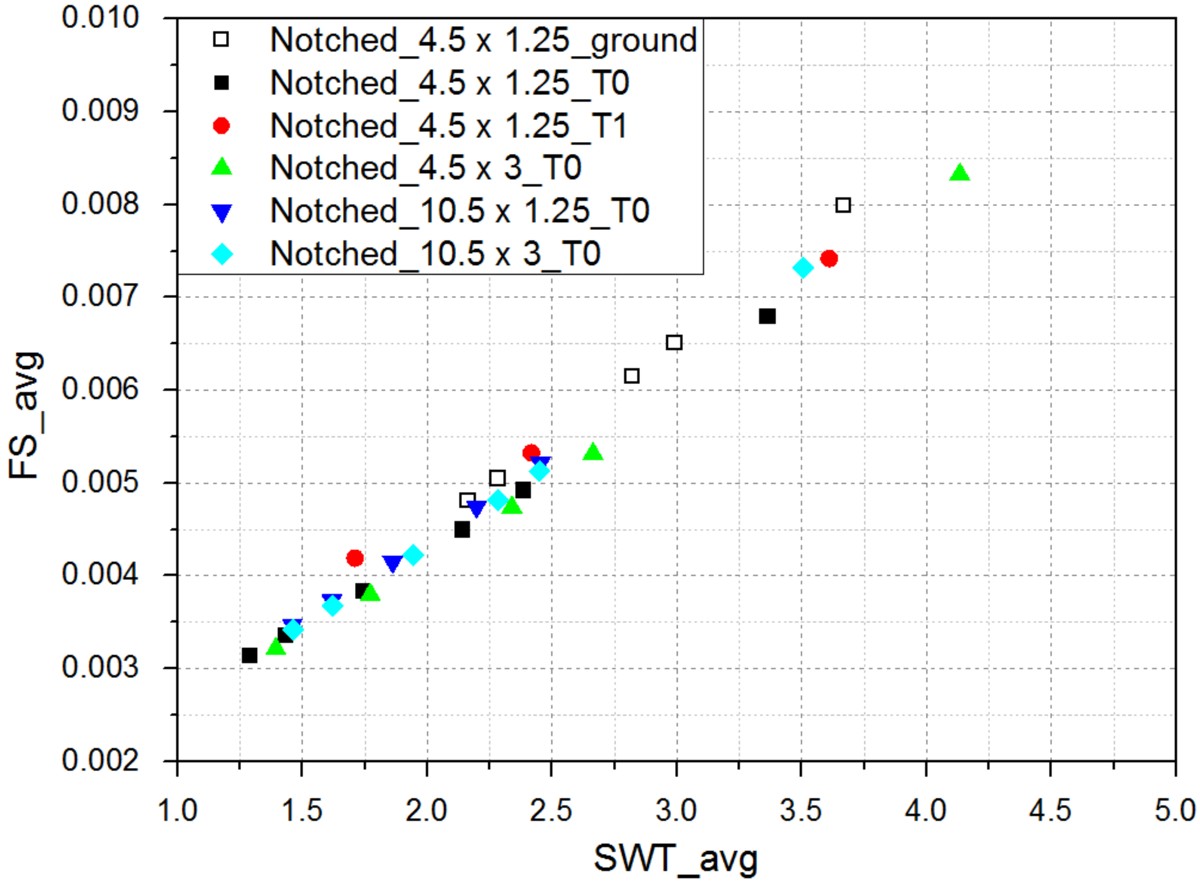

Fig. 11: Relation between the averaged SWT and FS parameters.

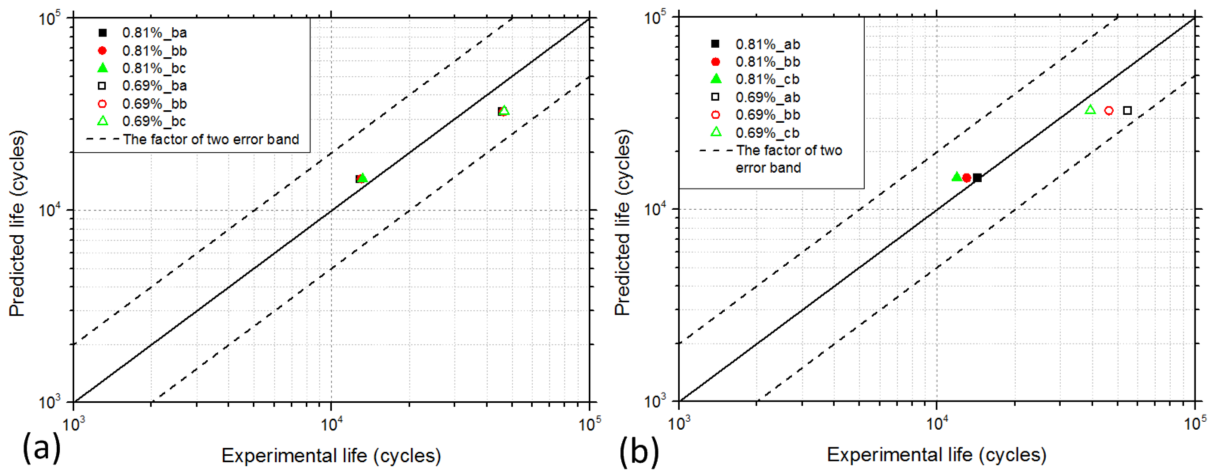

Fig. 12: The results of the sensitivity analysis for the SWT criteria; the effects of varying (a) strain hardening and (b) initial residual stress profiles on the accuracy of life predictions.